Chapter 10

Role of Interparticle Space in Hollow Spheres of Silica-Based Solid Acids on Their Acidic Properties and Activity for Hydrolytic Dehydrogenation of Ammonia Borane

Tetsuo Umegaki, Toyama Naoki and
Yoshiyuki Kojima

Additional information is available at the end of the chapter

http://dx.doi.org/10.5772/intechopen.71307

Abstract

Porous materials with micropores and mesopores have attracted much attention as materials potentially applied in various fields such as absorbents, catalysts, energy storage, and so on. The kind of materials showed intrinsic properties compared with other types of materials such as fine particles. This chapter reviewed our recent research about hollow silica-alumina composite spheres for the hydrolytic dehydrogenation of ammonia borane. This chapter has mainly discussed about the role of interparticle space in the hollow spheres on their acidic properties and activity for the hydrolytic dehydrogenation of ammonia borane.

Keywords: hollow spheres, interparticle space, silica-alumina, composite, hydrolytic dehydrogenation of ammonia borane

1. Introduction

The ability to generate highly defined, hierarchically structured materials that range in size from a few nanometers to several micrometers is a key prerequisite for the fabrication of highly functional materials. Such structured materials have potential applications in the fields of energy conversion, energy storage, catalysis, and separation [1–4]. Bottom-up approaches that rely on the self-assembly of molecular or colloidal building blocks into superstructures of defined length scales and symmetries have been used to obtain these structures [5, 6]. The size and shape of these building blocks translate directly into the

assembled superstructure [7, 8]. A small space made from pores or hollow structures leads to special properties such as the micropore filling of a pore for gas adsorption applications. If a special property were initiated into a solid-state material, a new possibility of material design would become available. Both porosity and hollow structures are very attractive for material functionalization.

Several papers have reported that mesoporous silica (MCM-41) itself acts as a typical acid catalyst for several reactions, including acetalization [9, 10], isomerization [11], and debenzylation [12]. Although the wall of mesoporous silica is made of amorphous silica and is generally believed to be neutral or slightly acidic, acetalization is generally believed to require strong or intermediate acids, such as HCl or proton zeolites, as catalysts [13–15]. These findings regarding the acidity of mesoporous silica [9–11, 16–21] raise important questions about how the surface of the material becomes acidic.

Hollow spheres have attracted much research and industrial interest due to their special shape, low density, and large fraction of voids. Hollow spheres possess a series of advantages such as tunable void volume, excellent flow performance, and large surface area. The large internal volume provides a storage space or artificial reaction cells that can serve many functions [22, 23]. The controlled synthesis of inorganic materials with well-designed structures at the nano-size level is extremely important in materials science. In particular, the preparation of hollow inorganic spheres with a defined structure has received increasing attention because of their broad potential applications ranging from drug delivery [24–26], ion exchange [27–29], sensors [30, 31], electro-optics [32, 33], and microreactors [34–36] to building block of photonic crystals [37]. Recently, this field has been advanced to the fabrication of hollow microspheres with holes on the shell wall, namely porous hollow microspheres. Because of their high specific surface area, low density, adsorption capacity, and ability to encapsulate actives, such materials are very useful in catalysis [38, 39], bioseparation [40, 41], tissue engineering [42–44], solar cells [45], and reaction separation [46].

In this chapter, we review our previous works of hollow silica-alumina composite spheres. In our previous study, we investigated fabrication and morphology control of the hollow spheres and functionality of the hollow spheres. First, we discussed intrinsic properties of the hollow spheres compared with the conventional fine particles and their morphological effects on their acidic properties and activity for hydrolytic dehydrogenation of ammonia borane. Second, we also discussed the influence of dispersion of active sites on activity of the hollow spheres for hydrolytic dehydrogenation of ammonia borane. Four-coordinated aluminum species substituting silicon atom in silica lattice was assigned as Brønsted acid sites, and the sites were active species for hydrolysis dehydrogenation of ammonia borane. Thus, the increase of their dispersion is expected to improve the activity of silica-alumina composite particles. From the above two points of view, we reviewed our previous works on hollow silica-alumina composite spheres.

http://dx.doi.org/10.5772/intechopen.71307

2. Typical experimental procedures

2.1. Preparation of composites

Hollow silica-alumina composite spheres were fabricated through the PS template method. Monodisperse PS particles were prepared by emulsifier-free emulsion polymerization using the following procedure. Styrene (9.0 mL; Kanto Chem. Co., >99.0%), poly(vinyl pyrrolidone) K30 (1.5 g; Fluka, Mw ≈ 40,000), and the cationic initiator 2,2′-azobis(2-metylpropionamidine) dihydrochloride (0.26 g; Wako Pure Chemical, >97.0%) were dissolved in ion exchanged water (100 mL) inside a 250-mL three-necked flask. The flask was equipped with a mechanical stirrer, a thermometer with a temperature controller, a nitrogen gas inlet, and a Graham condenser, and it was placed in an oil bath for heating. The reaction solution was deoxygenated by bubbling nitrogen gas at room temperature for 1 h and heated at 343 K for 24 h under stirring at 250 rpm. The final PS suspension was centrifuged at 6000 rpm for 5 min and washed three times with ethanol (30 mL; Kanto Chem.Co., >99.5%). The PS contents could be tailored through the addition of ethanol. Aluminum isopropoxide (0.0057 g; Aldrich, >98.0%), aqueous ammonia solution (3 mL; 28 wt.%, Kanto Chem. Co.), ethanol (40 mL), and tetraethoxysilane (0.1551 mL; TEOS, Kanto Chem. Co., >99.9%) were added to the PS suspension (15 g). The sol-gel reaction was carried out at 323 K for 1.5 h. The composite was dried overnight in a desiccator. Then, the composites were calcined in air at 873 K at a heating rate of 0.5 K min^{-1} and cooling down immediately after the designated temperature was reached. Fine silica-alumina composite particles were prepared by sol-gel method without the PS template particles. Aluminum isopropoxide (0.0057 g), aqueous ammonia solution (3 mL), and TEOS (0.1551 mL) were added to ethanol (40 mL). The sol-gel reaction was carried out at 323 K for 1.5 h. The composite was dried overnight in a desiccator. Then, the composite was calcined under the same conditions used for the hollow spheres.

2.2. Characterization

Morphology of the composite was identified by a transmission electron microscopy (TEM) using a Hitachi FE-2000 system operating at an acceleration voltage of 200 kV. Temperature-programmed desorption of ammonia (NH_3-TPD) was carried out on a BELCAT-B instrument. The analysis was performed by loading 50 mg of the composites into a quartz reactor and drying them under a flow of pure He at 783 K for 1 h followed by purging with pure He at the same temperature for 1 h. The composites were allowed to cool to 373 K under the He flow and then exposed to NH_3-He gas mixture (95 vol.% He) at 373 K for 1 h to allow NH_3 adsorption. The composites were then purged using pure He to allow for the accurate detection of the desorbed NH_3. The NH_3-TPD measurements were conducted by heating the composites from 373 to 773 K at a rate of 10 K min^{-1} under a flow of pure He. The desorbed NH_3 molecules were detected by a thermal conductivity detector (TCD).

2.3. Activity tests for hydrolytic dehydrogenation of NH_3BH_3

The composites were placed in a two-necked round-bottomed flask under air at room temperature. One of the necks was connected to a gas burette and the other was connected to an addition funnel. The reaction was initiated by adding aqueous NH_3BH_3 solution (3.5 mL, 0.14 wt.%; Aldrich, 90%) from the addition funnel to the composites. The evolution of gas from the reaction was monitored using the gas burette.

3. Results and discussion

3.1. Influence of the morphology on the activity for hydrolytic dehydrogenation of ammonia borane

Homogeneous hollow spheres of silica-alumina composite particles were obtained by adjusting some factors such as calcination temperature and soaking time [47]. **Figure 1a** shows TEM images of typical hollow silica-alumina composite spheres. Homogeneous hollow spheres with the shell thickness of ca. 6 nm and the particle size of ca. 220 nm were observed in the TEM image. The sample was prepared with PS templates with the diameter of ca. 200 nm; thus, the size of the hollow voids of the hollow spheres reflected the size of PS templates. The shell thickness and particle size were also controlled by adjusting ratios of silica-alumina composite to the amount of PS templates and particle size of PS templates, respectively [48–50]. **Figure 1b** shows the TEM image of the fine particles prepared with similar method for preparation of the hollow spheres without PS templates. The sample consists of fine particles with the particle size of ca. 13 nm. Particle agglomeration was observed in some parts of this composite. The specific surface areas of the hollow spheres and the fine particles were found to be 393 and 295 $m^2\ g^{-1}$, respectively, indicating that the specific surface areas do not significantly differ from each other, and the primary particles including the hollow spheres were slightly small compared with the particle size of the fine particles. On the other hand, both the hollow spheres and the fine particles consisted of a typical amorphous silica-alumina from the results of powder XRD measurements [51, 52].

The hollow silica-alumina composite spheres show unexpected high activity for hydrolytic dehydrogenation of ammonia borane compared with the silica-alumina composite

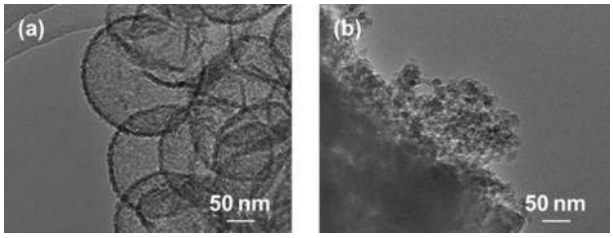

Figure 1. TEM images of (a) hollow silica-alumina composite spheres and (b) silica-alumina composite fine particles [52].

fine particles. The amount of evolved hydrogen from aqueous ammonia borane solution in the presence of the hollow spheres was 10 mL with the completion of the reaction in 12 min, while the evolution 2.5 mL of hydrogen with the completion of the reaction in 12 and 2 min, respectively. The molar ratios of the hydrolytically evolved hydrogen to the initial ammonia borane were 2.6 and 0.6 in the presence of the hollow spheres and the fine particles, respectively. These results indicate that the amount of hydrogen evolved in the presence of the hollow spheres was significantly higher than the amount of hydrogen evolved in the presence of the fine particles. It has been reported that the acidic protons on Brønsted acid sites promote the dissociation of the B–N bond and the hydrolysis of BH_3 species to produce borate ion species along with the hydrogen release Eq. (1) [47, 51, 53].

$$NH_3BH_3 + 2H_2O \rightarrow NH_4^+ + BO_2^- + 3H_2 \quad (1)$$

However, the hydrolytic dehydrogenation of ammonia borane in the presence of the hollow spheres was incomplete. It is suggested that the H_3BO_3 produced from the reaction of BO_2^- with the acidic protons on Brønsted acid sites shift the reaction shown in Eq. (2) to the right side [53].

$$H^+ + BO_2^- + H_2O \leftrightarrow H_3BO_3 \quad (2)$$

To determine the recycle ability of the composites, the activity of the recycled composites was compared. The recycled hollow spheres evolved 1.5 mL of hydrogen with the completion of the reaction in 2 min. On the other hand, the recycled fine particles showed no activity. The recycled hollow spheres were much lower amount of hydrogen evolution than the original hollow spheres because the acidic protons might be exchange into ammonium ion on the Brønsted acid sites of the hollow spheres during hydrolytic dehydrogenation of ammonia borane. Then, the recycled hollow spheres were calcined at 723 K at heating rate of 0.5 K min^{-1} and cooling down immediately after the designated temperature was reached. The recycled hollow spheres after calcination showed the same activity as the recycled hollow spheres. These results suggest that almost all the acidic protons on Brønsted acid sites of the hollow spheres were consumed by the hydrolytic dehydrogenation reaction. The acidic properties of the silica-alumina composites were measured using NH_3-TPD. **Figure 2** shows NH_3-TPD profiles of the hollow spheres and the fine particles. The NH_3 desorption from the hollow spheres showed two peaks: first peak at around 420 K (low-temperature peak) and a broad peak at around 580 K (high-temperature peak), whereas the NH_3 desorption from the fine particles showed peaks at around 420 and 430 K (low-temperature peaks), respectively. The low-temperature peaks can be attributed to Brønsted acid sites with weakly adsorbed NH_3 (weak Brønsted acid sites), whereas the high-temperature peak observed for the hollow spheres can be attributed to Brønsted acid sites with strongly absorbed NH_3 (strong Brønsted acid sites) [54–56]. These results indicate that the hollow spheres possess both weak and strong Brønsted acid sites, while the fine particles possess only weak Brønsted acid sites. The amount of Brønsted acid sites calculated from the areas under the peak in the temperature range 400–600 K [57–59] for the hollow spheres and the fine particles was 0.18 and 0.10 mmol g^{-1}, respectively. The result indicates that the amount of Brønsted acid sites

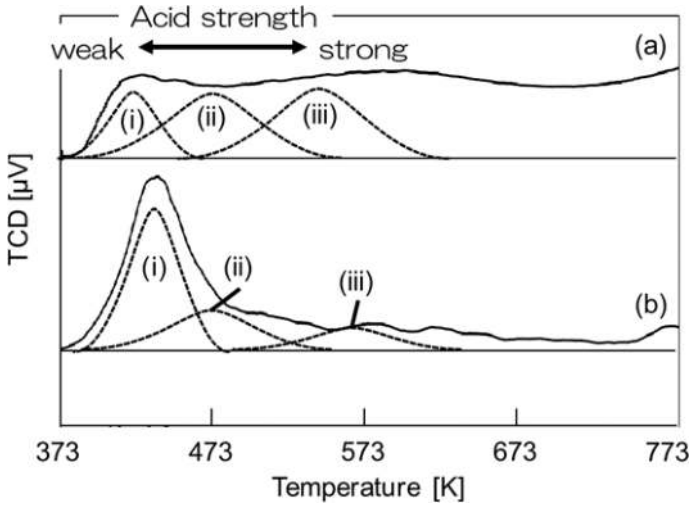

Figure 2. NH_3-TPD profiles of (a) hollow silica-alumina composite spheres and (b) silica-alumina composite fine particles [52].

in the silica-alumina composites depends on their morphology. According to the result, the amount of hydrogen evolution increases with the increase of the amount of Brønsted acid sites. The total amount of Brønsted acid sites in the hollow spheres is found to be 1.8 times higher than those in the fine particles. Moreover, the amount of hydrogen evolved in the presence of the hollow spheres is more than four times higher than that in the presence of the fine particles. Consequently, it is indicated that the morphology of silica-alumina composites influences their acidic properties and that the strong Brønsted acid sites are more effective for hydrolytic dehydrogenation of ammonia borane than the weak Brønsted acid sites. In addition, it is also suggested that the primary particles consisting of the shell of the hollow spheres formed micro- and/or meso-interparticles spacing, and the integrated surface acid sites showed unexpectedly strong acid property.

3.2. Improvement of dispersion of active species of hollow silica-alumina composite spheres

As described in the previous section, Brønsted acid sites are main active sites for hydrolytic dehydrogenation of ammonia borane. The acid sites can generally increase with the increase of four-coordinated aluminum species, which are well-dispersed active species. We investigated the influence of various preparation conditions such as promoters of sol-gel reaction for the formation of the shell of the hollow spheres, alcohol solvents, aluminum precursors, and so on, on the dispersion of the active aluminum species of hollow silica-alumina composite spheres and their activity for hydrolytic dehydrogenation of ammonia borane [60–62]. In the conditions, aluminum precursors significantly influenced on the dispersion and the activity. In this session, we especially introduce the investigation of the effects of aluminum precursors.

All the hollow silica-alumina composite spheres prepared using various aluminum precursors possessed similar morphology as shown in **Figure 3**. The shell thickness and diameter of all the hollow spheres were approximately 25 and 260 nm, respectively. The specific surface areas of the hollow spheres prepared using various aluminum precursors measured through nitrogen sorption using the Brunauer-Emmett-Teller (BET) methods were 436, 476, 483, and 523 $m^2\ g^{-1}$, respectively, indicating that the specific surface area does not significantly depend on the kind of aluminum precursors. On the other hand, the coordination numbers of the hollow spheres prepared using various aluminum precursors were quite different, and the ratio of four-coordinated aluminum species to all the aluminum species of the hollow spheres prepared using aluminum ethoxide, aluminum iso-propoxide, aluminum n-butoxide, and aluminum sec-butoxide calculated from the results of ^{27}Al MAS NMR spectra were 0.10, 0.33, 0.12, and 0.44, respectively [62]. The result indicates that the hollow spheres prepared using aluminum precursors with the branched alkyl groups exhibit larger proportion of four-coordinated aluminum species than those prepared using aluminum precursors with the normal alkyl groups. The dispersion of aluminum species increases with increase of the ratio of four-coordinated aluminum species [63]. The result indicates that the aluminum species of the hollow spheres prepared using aluminum precursors with the branched alkyl groups were well dispersed in the silica matrix. The acidic properties of the hollow spheres were measured using NH_3-TPD. **Figure 4** shows NH_3-TPD profiles of the hollow spheres prepared using various aluminum precursors. The assignment of NH_3 desorption peaks in this figure was same in Section 3.1, and the number of Brønsted acid sites was calculated using the area of the NH_3 desorption peaks of the hollow spheres. The number of Brønsted acid sites in the hollow spheres prepared using aluminum ethoxide, aluminum iso-propoxide, aluminum n-butoxide, and aluminum sec-butoxide were 0.08, 0.30, 0.12, and

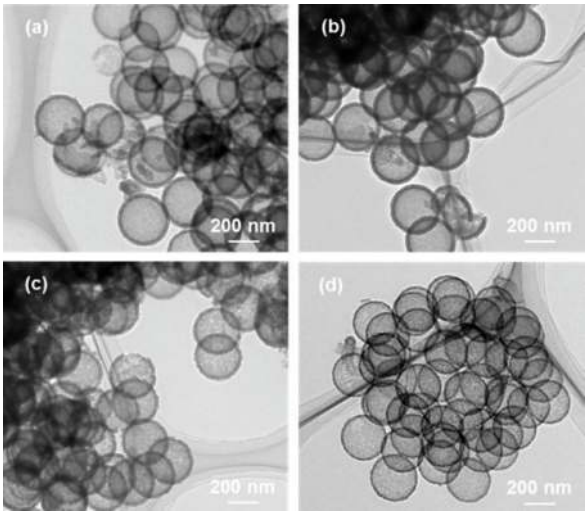

Figure 3. TEM images of hollow silica-alumina composite spheres prepared using (a) aluminum ethoxide, (b) aluminum iso-propoxide, (c) aluminum n-butoxide, and (d) aluminum sec-butoxide [62].

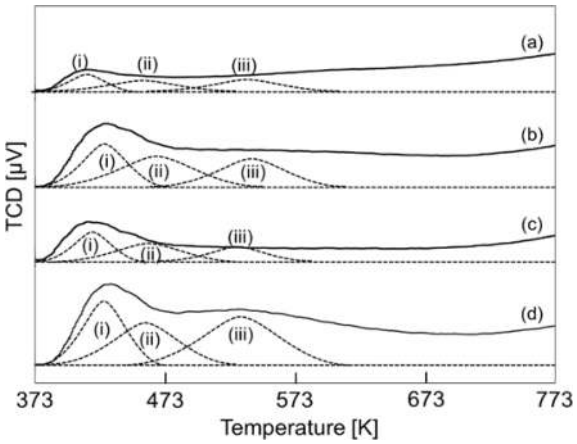

Figure 4. NH_3-TPD profiles of hollow silica-alumina composite spheres prepared using (a) aluminum ethoxide, (b) aluminum iso-propoxide, (c) aluminum n-butoxide, and (d) aluminum sec-butoxide [62].

0.34 mmol g^{-1}, respectively. From the result, the hollow spheres prepared using aluminum precursors with the branched alkyl groups exhibit more Brønsted acid sites than those prepared using aluminum precursors with the normal alkyl groups. The result indicates that the number of Brønsted acid sites depends on the kind of aluminum precursors. In addition, the surface concentrations of Brønsted acid sites in the hollow spheres prepared using aluminum ethoxide, aluminum iso-propoxide, aluminum n-butoxide, and aluminum sec-butoxide was 0.18, 0.63, 0.25, and 0.65 mmol m^2, respectively. From the result, the hollow spheres prepared using aluminum precursors with the branched alkyl groups exhibit more surface concentration of Brønsted acid sites than those prepared using aluminum precursors with the normal alkyl groups. The result suggests that the aluminum species of the hollow spheres prepared using aluminum precursors with the branched alkyl groups were well dispersed in the silica matrix.

The activities of the hollow spheres prepared using various aluminum precursors for hydrolytic dehydrogenation of ammonia borane were compared. The hydrogen evolution of 5.0, 10.5, 6.0, and 11.5 mL was occurred in 40, 45, 45, and 35 min, respectively, in the presence of the hollow spheres prepared using aluminum ethoxide, aluminum iso-propoxide, aluminum n-butoxide, and aluminum sec-butoxide, respectively. The molar ratios of the hydrolytically evolved hydrogen to introduced ammonia borane were 1.3, 2.8, 1.5, and 3.0 in the presence of the hollow spheres prepared using aluminum ethoxide, aluminum iso-propoxide, aluminum n-butoxide, and aluminum sec-butoxide, respectively. The hollow spheres prepared using aluminum precursors with the branched alkyl groups exhibit more hydrogen evolution than those prepared using aluminum precursors with the normal alkyl groups. It has been reported that the branched alkyl groups exhibit lower sol-gel reaction in silicon precursors rate than the normal alkyl groups because of steric effects [64]. Consequently, the amount of hydrogen evolution increases as the sol-gel reaction rate decreases. The result indicates that the amount of hydrogen evolution depends on the kind

of aluminum precursors. Hydrogen evolution of 1.0 mL was occurred in 3 min in the presence of the recycled hollow spheres prepared using aluminum sec-butoxide, indicating that the recycled hollow spheres exhibit much less hydrogen evolution than the fresh hollow spheres. The recycled hollow spheres prepared using aluminum ethoxide, aluminum iso-propoxide, and aluminum n-butoxide exhibit similar results. Hydrogen evolution rate of the hollow spheres prepared using aluminum ethoxide, aluminum iso-propoxide, aluminum n-butoxide, and aluminum sec-butoxide calculated using data from the first 50% of the reaction was 1.5, 2.0, 1.5, 2.0, and 0.3 mL min^{-1}, respectively, indicating that the rate of hydrogen evolution of all the hollow spheres was similar because they possess similar pore size distribution calculated from the results of nitrogen sorption measurement.

In order to evaluate the effect of the morphology and the dispersion of active aluminum species in the hollow spheres, the relation between the ratios of four-coordinated aluminum species and the activity for hydrogen evolution amount from aqueous solutions in the presence of various silica-aluminum composite particles. The relation calculated from some of our previous studies [52, 61, 62] was shown in **Figure 5**. From this figure, the hollow spheres showed unexpected high activity as compared with the fine particles, although the ratio of four-coordinated aluminum species in the hollow spheres was not significantly higher than the ratio of the fine particles. As described in Section 3.1, the larger amount of more effective strong Brønsted acid sites for hydrogen evolution from aqueous ammonia borane solution are in the hollow spheres than that in the fine particles. The micro- and/or meso-interparticles spacing formed by the primary particles in the shell of the hollow spheres in which the integrated surface acid sites showed unexpectedly strong acid property were included. On the other hand, the dispersion of aluminum species included in the hollow spheres was controlled by adjusting the preparation conditions and the activity for hydrogen evolution from aqueous ammonia borane solution linearly depended on the dispersion as shown in **Figure 5**.

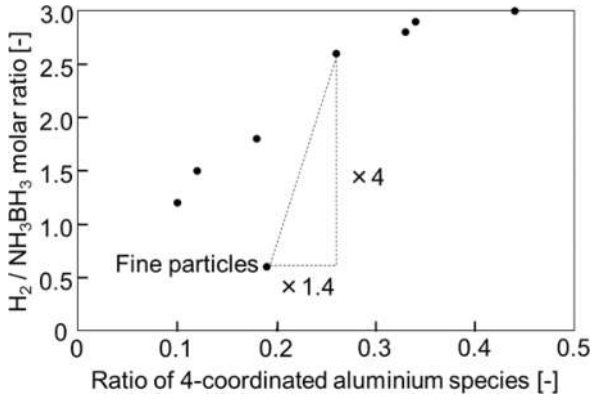

Figure 5. Relation between ratio of four-coordinated aluminum species and hydrogen evolution amount from aqueous ammonia borane solution in the presence of various silica-alumina composite particles [52, 61, 62].

4. Conclusions

In this chapter, we reviewed our previous works of fabrication and morphology control of the hollow spheres and functionality of the hollow spheres. The hollow silica-alumina composite spheres show unexpected high activity for hydrolytic dehydrogenation of ammonia borane compared with the silica-alumina composite fine particles though the ratio of active four-coordinated aluminum species of the hollow spheres was not significantly high compared with that of the fine particles. From the result of NH_3-TPD, the hollow spheres possessed higher number of strong Brønsted acid sites, which are effective for hydrolytic dehydrogenation of ammonia borane, than the fine particles. It possibly depends on micro- and/or meso-interparticles spacing, which was formed by the primary particles consisting of the shell of the hollow spheres, and it is suggested that the integrated surface acid sites showed unexpectedly strong acid property.

The activity of the hollow spheres for hydrolytic dehydrogenation of ammonia borane improved with increasing dispersion of active aluminum species and increasing four-coordinated aluminum species. We previously investigated the influence of various preparation conditions of the hollow spheres to improve the dispersion of the aluminum species and the activity for hydrolytic dehydrogenation of ammonia borane and aluminum precursor that significantly influence both on the dispersion and the activity. The number of Brønsted acid sites and ratio of four-coordinated aluminum species of the hollow spheres prepared using aluminum precursors with the branched alkyl groups was significantly higher than those of the hollow spheres prepared using aluminum precursors with the normal alkyl groups, and then the activity of the hollow spheres prepared using aluminum precursors with the branched alkyl groups was significantly higher than those of the hollow spheres prepared using aluminum precursors with the normal alkyl groups. These results indicate that the hollow spheres with well-ordered pore structure and well-dispersed active aluminum species are expected to show significantly high activity for the hydrogen evolution reaction.

Author details

Tetsuo Umegaki*, Toyama Naoki and Yoshiyuki Kojima

*Address all correspondence to: umegaki.tetsuo@nihon-u.ac.jp

College of Science and Technology, Nihon University, Tokyo, Japan

References

[1] Choi H, Sofranko AC, Dionysiou DD. Nanocrystalline TiO_2 Photocatalytic membranes with a hierarchical mesoporous multilayer structure: Synthesis, characterization, and multifunction. Advanced Functional Materials. 2006;**16**:1067-1074

[2] Rhee DK, Jung B, Kim YH, Yeo SJ, Choi SJ, Rauf A, Han S, Yi GR, Lee D, Yoo PJ. Particle-nested inverse opal structures as hierarchically structured large-scale membranes with tunable separation properties. ACS Applied Materials & Interfaces. 2014;**6**:9950-9954

[3] Su BL, Sanchez C, Yang XY. Hierarchically Structured Porous Materials: From Nanoscience to Catalysis, Separation, Optics, Energy, and Life Science. Weinheim: Wiley-VCH Verlag GmbH & Co. KGaA; 2011. ISSN: 978-3-527-32788-1

[4] Cho CY, Moon JH. Hierarchical twin-scale inverse opal TiO_2 electrodes for dye-sensitized solar cells. Langmuir. 2012;**28**:9372-9377

[5] Wang DY, Möhwald H. Template-directed colloidal self-assembly – The route to 'top-down' nanochemical engineering. Journal of Materials Chemistry. 2004;**14**:459-468

[6] von Freymann G, Kitaev V, Lotsch BV, Ozin GA. Bottom-up assembly of photonic crystals. Chemical Society Reviews. 2013;**42**:2528-2554

[7] Vogel N, Retsch M, Fustin CA, Del Campo A, Jonas U. Advances in colloidal assembly: The design of structure and hierarchy in two and three dimensions. Chemical Reviews. 2015;**115**:6265-6311

[8] Gröschel AH, Walther A, Löbling TI, Schacher FH, Schmalz H, Müller AHE. Guided hierarchical co-assembly of soft patchy nanoparticles. Nature. 2013;**503**:247-251

[9] Tanaka Y, Sawamura N, Iwamoto M. Highly effective acetalization of aldehydes and ketones with methanol on siliceous mesoporous material. Tetrahedron Letters. 1998;**39**:9457-9460

[10] Iwamoto M, Tanaka Y, Sawamura N, Namba S. Remarkable effect of pore size on the catalytic activity of mesoporous silica for the acetalization of cyclohexanone with methanol. Journal of American Chemical Society. 2003;**125**:13032-13033

[11] Yamamoto T, Tanaka T, Funabiki T, Yoshida S. Acidic property of FSM-16. Journal of Physical Chemistry B. 1998;**102**:5830-5839

[12] Itoh A, Kodama T, Maeda S. Masaki Y. Selective acceleration for deprotection of benzyl ethers with Ti-HMS. Tetrahedron Letters. December, 1998;**39**:9461-9464 ISSN 0040-4039

[13] Greene TW, Wuts PGM. Protective Groups in Organic Synthesis. 2nd ed. New York: John Wiley & Sons; 1991. p. 178

[14] Strukul G. Lewis acid behavior of cationic complexes of palladium(II) and platinum(II): Some examples of catalytic applications. Topics in Catalysis. 2002;**19**:33-42

[15] Urabe H, Sato F. In: Yamamoto H, editor. Lewis Acids in Organic Synthesis. Wiley-VCH: Weinheim; 2000. p. 653

[16] Thomas JM, Terasaki O, Gai PL, Zhou W, Gonzalez-Calbet J. Structural elucidation of microporous and Mesoporous catalysts and molecular sieves by high-resolution electron microscopy. Account of Chemical Research. 2001;**34**:583-594

[17] Trikalitis PN, Rangan KK, Bakas T, Kanatzidis MG. Varied pore organization in mesostructured semiconductors based on the $[SnSe_4]^{4-}$ anion. Nature. 2001;**410**:671-675

[18] On DT, Desplantier-Giscard D, Danumah C, Kaliaguine S. Perspectives in catalytic applications of mesostructured materials. Applied Catalysis A. 2001;**222**:299-357

[19] Lei C, Shin Y, Liu J, Ackerman EJ. Entrapping enzyme in a functionalized Nanoporous support. Journal of American Chemical Society. 2002;**124**:11242-11243

[20] Inagaki S, Guan S, Ohsuna T, Terasaki O. An ordered mesoporous organosilica hybrid material with a crystal-like wall structure. Nature. 2002;**416**:304-307

[21] Kageyama K, Tamazawa J, Aida T. Extrusion polymerization: Catalyzed synthesis of crystalline linear polyethylene nanofibers within a mesoporous silica. Science. 1999;**285**:2113-2115

[22] Meier W. Polymer nanocapsules. Chemical Society Reviews. 2000;**29**:295-303

[23] Caruso F. Hollow capsule processing through colloidal templating and self-assembly. Chemistry–European Journal. 2000;**6**:413-419

[24] Wei W, Ma GH, Hu G, Yu D, Mcleis T, ZG S, Shen ZY. Preparation of hierarchical hollow $CaCO_3$ particles and the application as anticancer drug carrier. Journal of American Chemical Society. 2008;**130**:15808-15810

[25] Moon SK, Oh MJ, Paik DH, Ryu TK, Park K, Kim SE, Park JH, Kim JH, Choi SW. A facile method for the preparation of monodisperse beads with uniform pore sizes for cell culture. Macromolecular Rapid Communication. 2013;**34**:399-405

[26] Zhu Y, Ikoma T, Hanagata N, Kaskel S. Rattle-type Fe_3O_4@SiO_2 hollow mesoporous spheres as carriers for drug delivery. Small. 2010;**6**:471-478

[27] Lou XW, Wang Y, Yuan C, Lee JY, Archer LA. Template-free synthesis of SnO_2 hollow nanostructures with high lithium storage capacity. Advanced Materials. 2006;**18**:2325-2329

[28] Cao AM, JS H, Liang HP, Wan LJ. Self-assembled vanadium pentoxide (V_2O_5) hollow microspheres from nanorods and their application in lithium-ion batteries. Angewande Chemie International Edition. 2005;**44**:4391-4395

[29] Lee KT, Jung YS, Oh SM. Synthesis of tin-encapsulated spherical hollow carbon for anode material in lithium secondary batteries. Journal of American Chemical Society. 2003;**125**: 5652-5653

[30] Gyger F, Hübner M, Feldmann C, Barsan N, Weimar U. Nanoscale SnO_2 hollow spheres and their application as a gas-sensing material. Chemistry of Materials. 2010;**22**:4821-4827

[31] Zhang J, Liu X, Wu S, Xu M, Guo X, Wang S. Au nanoparticle-decorated porous SnO_2 hollow spheres: A new model for a chemical sensor. Journal of Materials Chemistry. 2010;**20**: 6453-6459

[32] Jiang Y, Sun Q, Zhang L, Jiang Z. Capsules-in-bead scaffold: A rational architecture for spatially separated multienzyme cascade system. Journal of Materials Chemistry 2009;**19**: 9068-9074

[33] Wang Z, Wu L, Chen M, Zhou S. Facile synthesis of superparamagnetic fluorescent Fe_3O_4/ZnS hollow nanospheres. Journal of American Chemical Society. 2009;**131**:11276-11277

[34] Hyun DC, Lu P, Choi SI, Jeong U, Xia Y. Microscale polymer bottles corked with a phase-change material for temperature controlled release. Angewande Chemie International Edition. 2013;**52**:10468-10471

[35] Li M, Xue J. Facile route to synthesize polyurethane hollow microspheres with size-tunable single holes. Langmuir. 2011;**27**:3229-3232

[36] Im SH, Jeong U, Xia Y. Polymer hollow particles with controllable holes in their surfaces. Nature Material. 2005;**4**:671-675

[37] Xu X, Asher SA. Synthesis and utilization of monodisperse hollow polymeric particles in photonic crystals. Journal of American Chemical Society. 2004;**126**:7940-7945

[38] Tian G, Chen Y, Zhou W, Pan K, Dong Y, Tian C, Fu H. Facile solvothermal synthesis of hierarchical flower-like Bi_2MoO_6 hollow spheres as high performance visible-light driven photocatalysts. Journal of Materials Chemistry. 2011;**21**:887-892

[39] Chen Q, Bahnemann DW. Reduction of carbon dioxide by magnetite: Implications for the primordial synthesis of organic molecules. Journal of American Chemical Society. 2000;**122**:970-971

[40] Kirkland J, Truszkowski F, Dilks Jr C, Engel G. Superficially porous silica microspheres for fast high-performance liquid chromatography of macromolecules. Journal Chromatography A. 2000;**890**:3-13

[41] Qu JB, Wan XZ, Zhai YQ, Zhou WQ, Su ZG, Ma GH. A novel stationary phase derivatized from hydrophilic gigaporous polystyrene-based microspheres for high-speed protein chromatography. Journal of Chromatography A. 2009;**1216**:6511-6516

[42] Kim SE, Park JH, Cho YW, Chung H, Jeong SY, Lee EB, Kwon IC. Porous chitosan scaffold containing microspheres loaded with transforming growth factor-β1: Implications for cartilage tissue engineering. Journal of Controlled Release. 2003;**91**:365-374

[43] Langer R, Tirrell DA. Designing materials for biology and medicine. Nature. 2004;**428**:487-492

[44] Hollister SJ. Porous scaffold design for tissue engineering. Nature Material. 2005;**4**:518-524

[45] Bach U, Lupo D, Comte P, Moser J, Weissörtel F, Salbeck J, Spreitzer H, Grätzel M. Solid-state dye-sensitized mesoporous TiO_2 solar cells with high photon-to-electron conversion efficiencies. Nature. 1998;**395**:583-585

[46] Fan JB, Huang C, Jiang L, Wang S. Nanoporous microspheres: From controllable synthesis to healthcare applications. Journal of Materials Chemistry B. 2013;**1**:2222-2235

[47] Toyama N, Umegaki T, Kojima Y. Fabrication of hollow silica-alumina composite spheres and their activity for hydrolytic dehydrogenation of ammonia borane. International Journal of Hydrogen Energy. 2014;**39**:17136-17143

[48] Toyama N, Umegaki T, Xu Q, Kojima Y. Control of shell thickness of hollow silica-alumina composite spheres and their activity for hydrolytic dehydrogenation of ammonia borane. Key Engineering Materials. 2014;**617**:166-169

[49] Toyama N, Umegaki T, Xu Q, Kojima Y. Control of particle size of hollow silica-alumina composite spheres and their activity for hydrolytic dehydrogenation of ammonia Borane. Journal of Japan Institute of Energy. 2014;**93**:511-516

[50] Toyama N, Kamada K, Umegaki T, Kojima Y. Control of particle size of hollow silica-alumina composite spheres prepared using L(+)-arginine and their activity for hydrolytic dehydrogenation of ammonia borane. Transactions of Materials Research Society of Japan. 2015; **40**:81-84

[51] Toyama N, Umegaki T, Kojima Y. Influence of Si/Al molar ratio of hollow silica-alumina composite spheres on their activity for hydrogenation dehydrogenation of ammonia borane. International Journal of Hydrogen Energy. 2015;**40**:6151-6157

[52] Toyama N, Ohki S, Tansho M, Shimizu T, Umegaki T, Kojima Y. Influence of morphology of silica-alumina composites on their activity for hydrolytic dehydrogenation of ammonia Borane. Journal of Japan Institute of Energy. 2016;**95**:480-486

[53] Chandra M, Xu Q. Dissociation and hydrolysis of ammonia-borane with solid acids and carbon dioxide: An efficient hydrogen generation system. Journal of Power Sources. 2006;**159**:855-860

[54] Topsøe NY, Pedersen K, Derouane E. Infrared and temperature-programmed desorption study of the acidic properties of ZSM-5-type zeolites. Journal of Catalysis. 1981;**70**:41-52

[55] Hidalgo CV, Itoh H, Hattori T, Niwa M, Murakami Y. ESCA studies on silica- and alumina-supported rhenium oxide catalysts. Journal of Catalysis. 1984;**85**:362-369

[56] Tonetto G, Atias J, de Lasa H. FCC catalysts with different zeolite crystallite sizes: Acidity, structural properties and reactivity. Applied Catalysis A. 2004;**270**:9-25

[57] Fang X, Liu Z, Hsieh MF, Chen M, Liu P, Chen C, Zheng N. Hollow Mesoporous Aluminosilica spheres with perpendicular pore channels as catalytic nanoreactors. ACS Nano. 2012;**6**:4434-4444

[58] Sakthivel A, Dapurkar SE, Gupta NM, Kulshreshtha SK, Selvam P. The influence of aluminium sources on the acidic behaviour as well as on the catalytic activity of mesoporous H-AlMCM-41 molecular sieves. Microporous and Mesoporous Materials. 2003;**65**:177-187

[59] Wang Y, Lang N, Tuel A. Nature and acidity of aluminum species in AlMCM-41 with a high aluminum content (Si/Al = 1.25). Microporous and Mesoporous Materials. 2006;**93**:46-54

[60] Umegaki T, Imamura S, Toyama N, Kojima Y. Influence of preparation conditions on the morphology of hollow silica–alumina composite spheres and their activity for hydrolytic dehydrogenation of ammonia borane. Microporous and Mesoporous Materials. 2014;**196**: 349-353

[61] Toyama N, Ohki S, Tansho M, Shimizu T, Umegaki T, Kojima Y. Influence of alcohol solvents on morphology of hollow silica–alumina composite spheres and their activity for hydrolytic dehydrogenation of ammonia borane. Journal of Sol-Gel Science and Technology. 2017;**82**:92-100

[62] Toyama N, Ohki S, Tansho M, Shimizu T, Umegaki T, Kojima Y. Influence of aluminum precursors on structure and acidic properties of hollow silica-alumina composite spheres, and their activity for hydrolytic dehydrogenation of ammonia borane. International Journal of Hydrogen Energy. 2017;**42**:22318-22324

[63] Koekkoek AJJ, Rob van Veen JA, Gerrtisen PB, Giltay P, Magusin PCMM, Hensen EJM. Brønsted acidity of Al/SBA-15. Microporous and Mesoporous Materials. 2012;**151**:34-43

[64] Brinker CJ. Hydrolysis and condensation of silicates: Effects on structure. Journal of Non-Crystalline Solids. 1988;**100**:31-50